



Recent trend in controlling root rot disease of tomato caused by *Fusarium Solani* using aluminasilica nanoparticles

M. Shenashen¹; A. Derbalah^{1,2*}; A. Hamza²; A. Mohamed³, S. El Safty^{1,4}

¹National Institute for Materials Science (NIMS) 1-2-1 Sengen, Tsukuba-shi, Ibaraki-ken, 305-0047 (Japan)

²Pesticides Chemistry and Toxicology Department, Faculty of Agriculture, Kafr-El-Shiekh University, 33516 Egypt

³ Plant Pathology Research Institute, Agriculture Research Centre, Giza, Egypt

⁴Graduate School for Advanced Science and Engineering, Waseda University 3-4-1 Okubo, Shinjuku-ku, Tokyo 169-8555 (Japan)

*Corresponding Author

*Professor. **Aly Soliman Hamed Derbalah**

Pesticides Chemistry and Toxicology Department, Faculty of Agriculture, Kafr El-Sheikh Univ. 33516, Kafr El-Sheikh, Egypt Phone: 20473255831 Fax: 20473232032

E-mail: aliderbalah@yahoo.com

Abstract

This study was carried out to synthesis of mesoporous aluminasilica nanoparticles (MASN) and to evaluate its antifungal activity against root rot of tomato caused by *Fusarium solani* under laboratory and greenhouse conditions compare to recommended fungicide (chinosol). The effect of MASN on some growth characters was also investigated. The physical characteristics of MASN, such as porosity, surface area, and pore volume contributed to its high antifungal efficacy toward *Fusarium solani*. Chinosol and aluminasilica were effective against *Fusarium solani* under both laboratory and greenhouse conditions. MASN nanoparticles were potentially effective against root rot of tomato but further studies on its efficacy under field conditions and improving its synthesis characters are needed.

Keywords: Alumina silica, control, nanoparticles, root rot, tomato

Introduction

Tomato is considered as a remarkable vegetable crop due to its economic importance and nutritional value (Giovannucci, 1999). Tomato is planted in most countries either in open field or greenhouse vegetation. In other countries, such as Egypt, tomato is considered as a main vegetable crop used for food and industrial purposes (EL-Mougy, 1995).

Various microorganisms are involved in creating pests in agriculture sector. Among these microorganisms, fungi hold a remarkable share, such that the percentage of diseases caused by fungi in agricultural systems is very high (Hadian et al., 2011). Plants are usually attacked by numerous diseases caused by fungi, bacteria, and viruses that induce large losses to cultivars (Esfahani, 2006). *Fusarium* fungus is a

significant plant pathogen found in various kinds of crops.

Controlling and coping with plant diseases are among the most crucial challenges in the agriculture sector. Various traditional procedures have been used to control plant diseases with one or more restrictions. For example, chemical fungicides severely impact the environment and humans.

Recent improvements on nanotechnology science, especially in the preparation of arranged nanoparticles with specific size and shape, results in the detection of novel bio-agents with pesticidal activity. Therefore, eco-friendly and low cost nanomaterials were considered as alternatives to chemical fungicides for the control of plant diseases (Kumar and Yadav, 2009). The popularity of metallic nanoparticles (NPs) increased nowadays because of their significant properties. Using the design of novel nanomaterials and considering their surface forms, we can determine their antimicrobial potential to alleviate or prohibit fungal growth for medical and agricultural aims.

Nanomaterials and mesoporous materials provide a good molecular support in diverse potential applications related to their unique properties, such as geometrical order, tunable size, and high stability under various environment phases (EL-Safty et al., 2008; EL-Safty et al., 2012). Fabrication and design of mesoporous materials, which display order and connectivity of mesopores and high surface area, may offer potential applications for chemical capture and analysis in environmental and medical fields (Platschek et al., 2006; EL Safty et al., 2010; Khairy and EL-Safty, 2014). The development of efficient, low-cost, and reproducible mesoporous materials for each specific application is still a challenge. Inorganic oxide powders possess a massive amount of active sites, which can significantly accelerate the hydrolysis process. Hence, in this context, inorganic oxide powders may treat well with these demands. The conjunction of aluminum atoms in the framework of mesopore aluminasilica is considered as one of the main reasons for creating acidic active sites; such acidity is considered a major factor in different material applications (Che et al., 2003; EL-Safty et al., 2003; Garcia-Bennett et al., 2006; Wang et al., 2006; EL Safty et al. 2013). Nevertheless, many different applications in our daily lives, such as catalysis processes, sensor design, and membrane filtration, are based on the use of aluminosilica

materials (Climent et al., 1996; EL-Safty et al., 2008; Zukal et al., 2010).

Current work report the effect of mesoporous aluminasilica nanoparticles (MASN) with large, tunable, and open cylindrical pores as potential antifungal agent to root rot of tomato caused by *Fusarium solani*. The effect of MASN on tomato growth (plant height, as well as fresh and dry weight) compare to chinisol fungicide was also evaluated.

Materials and Methods

Chemicals

All chemicals used for metal oxide synthesis were highly purified. Tetramethylorthosilicate (TMOS), aluminum nitrate nonahydrate ($\text{Al}(\text{NO}_3)_3 \cdot 9\text{H}_2\text{O}$), aluminum chloride hexahydrate ($\text{AlCl}_3 \cdot 6\text{H}_2\text{O}$), dodecane ($\text{C}_{12}\text{H}_{26}$), and the triblock copolymers of poly (ethylene oxide-b-propylene oxide-b-ethylene oxide, Pluronic P123), designated as P_{123} ($\text{EO}_{20}\text{PO}_{70}\text{EO}_{20}$) were purchased from Sigma-Aldrich Company, Ltd. USA. The recommended compound for tomato root rot Chinisol was obtained from Probelte, S.A. Company Spain.

Synthesis of MASN

Cubic Ia3d aluminasilica were fabricated using simple one-pot microemulsion polymerization technique in conjunction with sol-gel process, according to previous fabrication method reported for HOM silica monoliths (EL-Safty et al., 2013; Shenashen et al., 2013a; Shenashen et al., 2015).

Characterization instruments

To investigate and analyze the surface properties, such as specific surface area and the pore structure of the prepared materials, Belsorp MINI-II analyzer (JP. BEL Co. Ltd) at 77 K was used to determine the N_2 adsorption-desorption isotherms. The Barrett-Joyner-Halenda (BJH) analysis of the adsorption isotherm curve was used to confirm the cylindrical pore diameter of the monolithic material. Pretreatment of the sample was conducted at 200 °C for 8 h with an equilibrated pressure of 10^{-3} Torr.

Small/wide-angle XRD patterns were recorded on a 18 kW diffractometer (Bruker D8 Advance) using Cu K radiation, conducted in the range of 0.1° – 6.5° . DIFFRAC plus Evaluation Package (EVA) software was used to analyze the diffraction data based on the

databases of the International Centre for Diffraction Data (Kern et al., 2004; Shenashen et al., 2013b).

Transmission electron microscopy (TEM) analysis was used to evaluate the porosity for the fabricated material. The macro-structure of the prepared material was measured using a Hitachi S-4300 field-emission scanning electron microscope (SEM). ^{29}Si MAS NMR spectra were carried out on a Bruker AMX-500 spectrometer. The ^{29}Si MAS NMR spectra were analyzed at 125.78 MHz with a pulse length of 4.7 μs . ^{27}Al NMR spectra were operated at 125.78 MHz with a 90° pulse length of 4.7 μs . NH_3 Temperature-Programmed Desorption (NH_3 -TPD) was used to investigate the acidity of the aluminasilica materials using BEL-Japan TPD-1S system with a quadrupole mass spectrometer.

Isolation, identification and culturing of *F. solani*

Samples of tomato plants exhibiting root rot symptoms were collected from various infected areas. The plant samples with their rhizosphere soil were placed in polyethylene pockets and conveyed to the laboratory for further treatment. To remove all soil particles attached the lower parts of stems and roots of tomato plants; tap water was used for washing it. The samples were then cut into small pieces (approx. 2 cm). Then, the small surface parts were sterilized by 3% sodium hypochlorite for 3 min and washed many times using sterilized distilled water. Thereafter, they were dried using two clean filter papers. The cleaned small parts were then placed onto potato dextrose agar (PDA) medium, and kept at 27–30 °C for 3–5 days. The hyphal tip technique was used to purify the growing fungal colonies on the PDA medium (Dhingra and Sinclair, 1995).

The fungus was identified according to the morphological and microscopical characters following the description given by Ainsworth and James (1971) and Alexopolous et al., (1996) at the Mycology Research and Survey of Plant diseases Section, Plant Pathology Research Institute, Agriculture Research Center, Giza, Egypt. After that culture of identified *F. solani* were grow independently on hull rice medium. Cultured plates of fungal isolate were observed for macroscopic characteristics such as colony diameter, exudates, colony reverse and microscopic characteristics including conidiophores, vesicle, metulae, phialides and conidia. For microscopic characteristics slides were stained with cotton blue and mounted in lectophenol. Photographs were taken with digital

camera Canon Power Shot A550, 7.1 mega pixels. A morphological examination of species was first made with naked eye and at low magnification power of microscope after that detailed examination was done according to Ainsworth and James (1971) by measuring the dimensions of the microscopic structures, photographing the microscopic structures and using relevant literature as reference.

Culture of *F. solani* was grown separately on a rice hull medium. Glass bottles (500 ml), each containing 100 g rice hulls, 200 g sand, and water (100 ml), were sterilized in an autoclave and incubated for 20 min at a pressure of 1.5 atm. Thereafter, the bottles of the medium were inoculated separately by adding three mycelial disks (6 mm in diameter) taken from the growing colony of the fungal isolate on PDA. The glass bottles with rice hull culture were incubated at 20–28 \pm 2 °C for seven days.

Screening of MASN antifungal activity against *F. solani*

The efficacy of MASN and Chinosol were evaluated against *F. solani* under laboratory conditions. The antifungal activity of was determined as the percent of inhibition in the growth relative to the control treatment. PDA spiked with MASN and chinosol at concentrations of 100, 150, 200, 300, and 400 mg/l was poured into Petri dishes (9 cm diameter) at a rate of 15 ml/dish. The dishes inoculated in the center with a disk of *F. solani* culture (five day old culture). A sterilized liquid medium without the tested treatments was added into used as the control. Parafilm was used to close the plates to reduce the evaporation of the tested materials. The incubation time for the plates at 28 °C was extended until the full growth of *F. solani* (mycelium reaching the edge of the plate) in the untreated control group. The formula suggested by Vincent (1947) was used to calculate the percentage of inhibition in the radial growth of *F. solani*. Every treatment was replicated five times. The inhibition percentage was calculated as shown in the following equation:

$$\text{Inhibition (\%)} = A - B/A \times 100$$

where A = the radial growth control and B = the radial growth in treatment.

Efficacy of MASN under greenhouse conditions

The efficacy of MASN on fusarium root rot caused by *F. solani* compared with chinisol was estimated under greenhouse conditions. Sandy-clay soil was sterilized using a formalin solution of 5%, then compacted into 25 cm diameter pots, 4 kg soil/pot. Artificial inoculation was carried out in pots one week before sowing at a rate of 3% using the rice hull culture (w/w) and kept moist until sowing. Roots of tomato seedlings (cv. Super Strain B) with age of 25 days old were treated by dipping for 2 h in a solution of MASN and chinisol separately (EL-Mohamedy et al., 2014). Roots of tomato seedlings were treated with MASN and the recommended fungicide by preparing aqueous solution at the most effective concentration (400 mg/L) under laboratory conditions. For the control treatment, roots of tomato seedlings were dipped in distilled water for 2 h. Each treatment was represented by five replicates. Afterward, the tomato seedlings were transplanted to inoculated soil with *F. solani* in the pots with 5 plants to each pot. Some growth characters (plant height and fresh and dry weights) of tomato plant were measured in the second season. The efficacy of the MASN and chinisol was assessed by calculating the percentage of survived plants (healthy

plants in a good conditions without disease symptoms) that were registered 45 days after sowing using the following equation described by Khalifa (1987)

$$\text{Survived plants (\%)} = \frac{\text{No. of survived plants}}{\text{No. of sown seeds}} \times 100.$$

Statistical analysis

Statistical analysis for the data was performed with JMP soft-ware version 8 using the Turkey Kramer HSD test for determining significant differences among treatment at P = 0.05 level. Each experiment was repeated twice and each treatment consisted of four replicates.

Results

Characterization of MASN antifungal agent

The XRD patterns of synthesized aluminasilica are shown in (Fig. S1A). Mesoporous aluminasilica presents clear diffraction peak at 0.94° . This can be indexed as (211) diffraction planes, which is a feature of highly ordered cubic Ia3d nanophase domains (Fig. S1A).

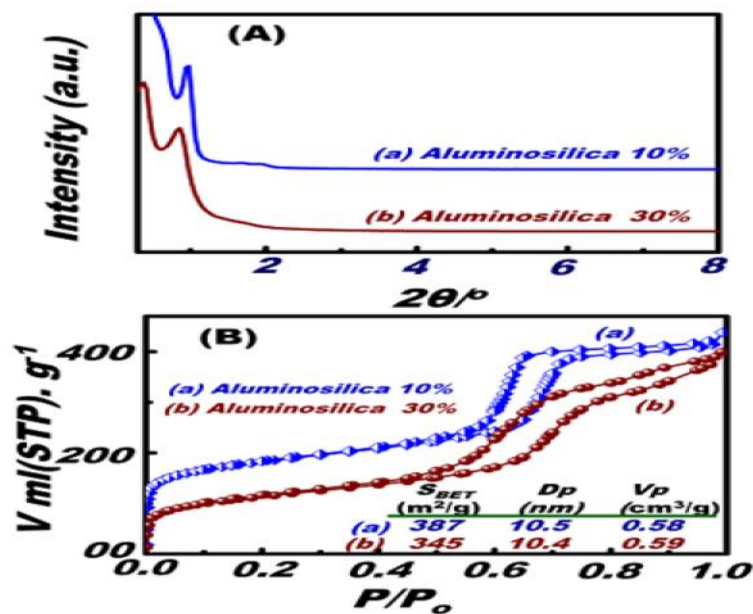


Fig.S1 SAXS (A) and nitrogen isotherms (B) of aluminasilica 10% (a) and aluminasilica 30% monoliths (b)

The N_2 adsorption isotherms of the monolith fabricated materials are shown in Fig.S 1B. The isotherm curves elucidated the presence of type-IV with H1 hysteresis loop matched with the properties of cylindrical mesoporous materials (EL-Safty et al., 2005; EL-Safty et al., 2013; EL-Safty et al., 2015). During dealumination process by calcination, the

aluminum might immigrate and stabilize in the surface, thereby forming a separate species of aluminum (Shen and Kawi, 1999). On the other side, the mesopore/micropore volumes and surface areas were decreased in case of low Si/Al ratios. This decrease was due to the degradation of the mesopore's regularity (Lippmaa et al., 1986; Lambert et al.,

1989). The textural parameters, such as BET surface area (S_{BET}), pore volume (V_p), and average pore size (D_p), are shown in Fig. S1B and S1B inset. The small decrease in the S_{BET} and V_p is a result of increasing the aluminum contents. S_{BET} of aluminasilica 10% and aluminasilica 30% were found to be 387 and 345 m^2/g , respectively. V_p of aluminasilica 10% and aluminasilica 30% were found to be 0.58 and 0.59 cm^3/g , respectively. Moreover, D_p of aluminasilica 10% and aluminasilica 30% were found to be 10.5, and 10.4 nm, respectively.

The crystallinity and effect of the alumina content on the degree of aluminasilica relative to crystallinity was

studied using wide-angle powder XRD technique. Fig. S2 exhibited the wide-angle powder X-ray diffraction of treated cubic Ia3d aluminasilica monoliths at a higher temperature of 800 °C. The XRD analysis of aluminasilica 30% confirmed the disordered local structure as congruous with the powdery mesoporous aluminasilica (Fig. S2b). However, in case of aluminasilica 10%, the XRD patterns confirmed the formation of crystalline alumina matrices, as seen from the well-resolved and distinguished peaks (Fig. S2a) (Lui et al., 2000; Du et al., 2002; Linssen et al., 2003; Shigeno et al., 2003).

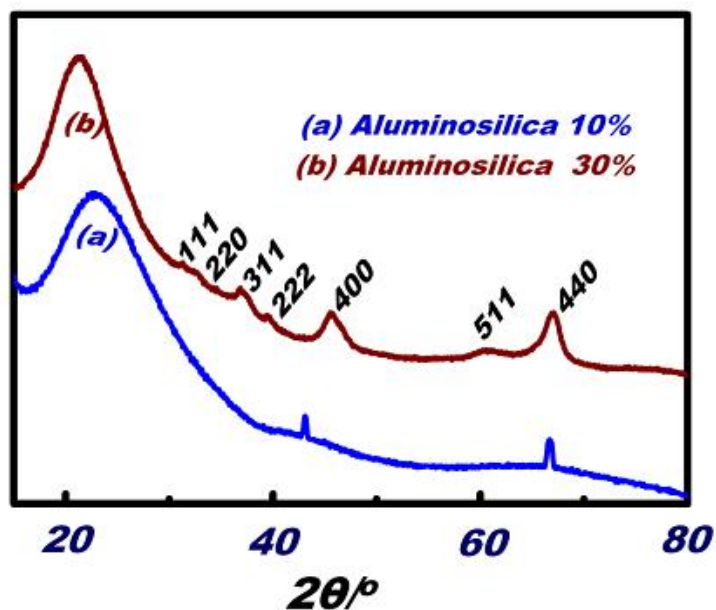


Fig.S2 Representative XRD patterns of calcined cubic Ia3d aluminasilica 10% (a) and aluminasilica 30% (b) monoliths

SEM micrographs of the aluminasilica monoliths display the morphological particle stability of monolithic materials (Fig. S3). Apparently, the monolith particles exhibited a micrometer-sized shape and were formed by the aggregation of large amounts

of nanoparticles of Al composition. However, SEM images revealed that some of the open pore structures comprised not very well-defined cavities circumfluent with irregular alumina.

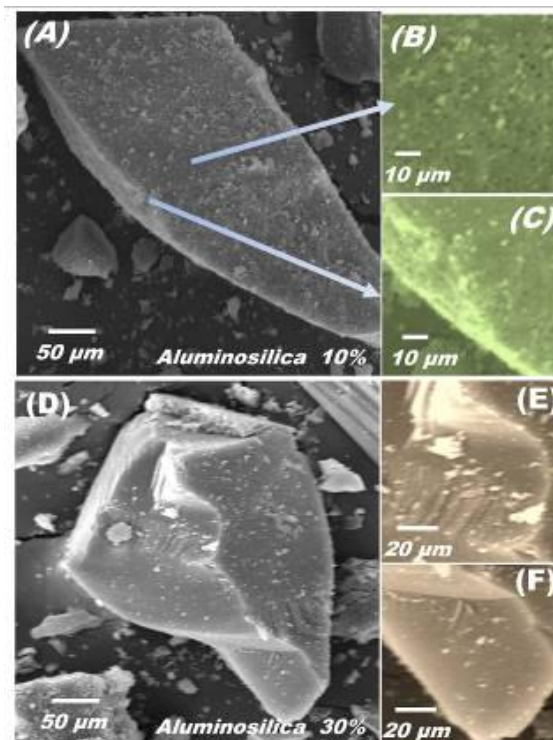


Fig. S3 Representative HRSEM micrographs of calcined cubic Ia3d aluminasilica 10% (A–C) and aluminasilica 30% monoliths (D–F)

Clearly, the main features of the fabricated and designed materials inclusive of the retention of elevated average of 3D ordering, particle size in micrometric range, and desirable distribution of the target into the mesopore surfaces architectures have been confirmed by the TEM and SEM micrographs, as well as SAXS and N₂ isotherm profiles (Figs. S1–3). The TEM images of aluminasilica 10% and aluminasilica 30% monoliths were recorded along the directions of 110 and 111, respectively (Fig.S 4).

Regular and well-defined order of the mesopore channels over all the directional arrays was observed. Fig. S4 insets are the corresponding ED pattern analyses that reveal the formation of ordered aluminasilica 10% and aluminasilica 30% monoliths in agreement with the well-defined XRD analysis. The mesopore uniformity in the monolith framework was virtually affected by the aluminum contents as observed in TEM micrographs.

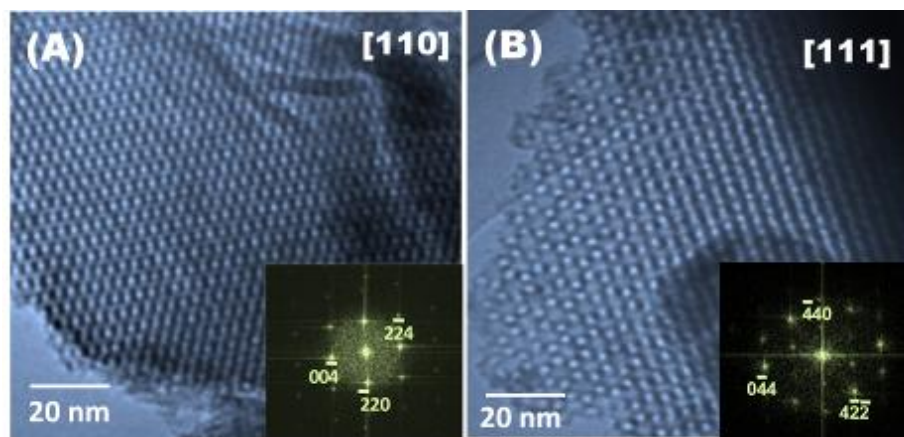


Fig. S4 Representative HRTEM and FTD (insets) images of the aluminasilica 10% (A) and aluminasilica 30% (B)

To evaluate the nature of the aluminasilica materials, ^{27}Al NMR and ^{29}Si solid-state NMR spectroscopies were used (Fig.S 5). The ^{29}Si NMR spectra of calcined aluminasilica samples display the presence of three peaks related to different silicon species (Fig. S5A). The three resolved peaks of the aluminasilica sample at chemical shift () were -85 , -98 , and -106 ppm, in which these features can be readily assigned to the $\text{Si}(\text{OSi})_2$ ($\text{OAl})_2$ (Q_2), $\text{Si}(\text{OSi})_3$ ($\text{OAl})$ (Q_3), and $\text{Si}(\text{OSi})_4$ (Q_4) species, respectively (Shenashen et al., 2013c). The main resonance peak at -98 ppm related to Q_3 , whereas the two shoulders at -106 and -85 ppm related to Q_4 and Q_2 , respectively; these were observed

after the calcination process. In fact, the obtained data of the NMR are consistent with the previous reports of aluminasilica structures (EL-Safty et al., 2012).

^{27}Al NMR spectra were used to assess the coordination types and location of different aluminum sites in the monolithic aluminasilica (Fig. S5B). The samples showed two ^{27}Al chemical shifts, namely, a sharp resonance at -1 , which is related to octahedral aluminum (Al^{VI} , AlO_6 , extra-framework) and a small resonance at 58 ppm that indicates the existence of the tetrahedral (Al^{IV} , AlO_4 , framework) (Fig. S5B).

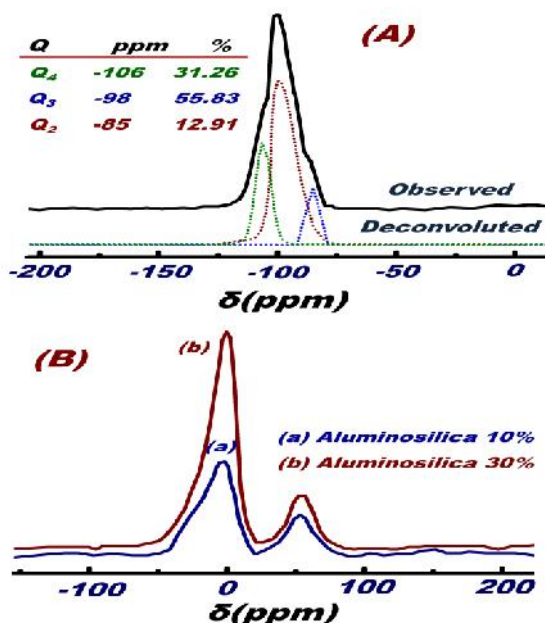


Fig. S5 ^{29}Si MAS NMR spectra of calcined monolithic cubic Ia3d aluminasilica 30% (A), and ^{27}Al MAS NMR spectra (B) of calcined cubic Ia3d aluminasilica 10% (a) and aluminasilica 30% (b).

Temperature-programmed desorption of ammonia (NH_3 -TPD) was used to test the acidity and basicity centers of the materials (Fig. 6). As shown in Fig. S6, the NH_3 -TPD profiles of the samples show two types of NH_3 desorption. The first type was at around 200 $^\circ\text{C}$, which indicated desorption of ammonia from weak acid sites. The second was in the range 400 – 500 $^\circ\text{C}$, which was a broad peak related to desorption of ammonia from mildly strong acid sites of monolithic aluminasilica (Xia et al., 2006, Derbalah et al., 2015). An increase in the peak area associated with the

increase of aluminum content was observed. Further investigation on the reasons behind the change of acid type and amount was carried out using ^{29}Si MAS NMR and ^{27}Al MAS NMR (Fig. 5). It is necessary to observe the presence of a weak shift in the weak acid position "from 200 to 180 $^\circ\text{C}$ " by increasing aluminum content. This shift confirms the presence of high acidity sites leading to the fast kinetic of adsorbate (NH_3) accessibility (Bai et al., 2009; Das et al., 2009).

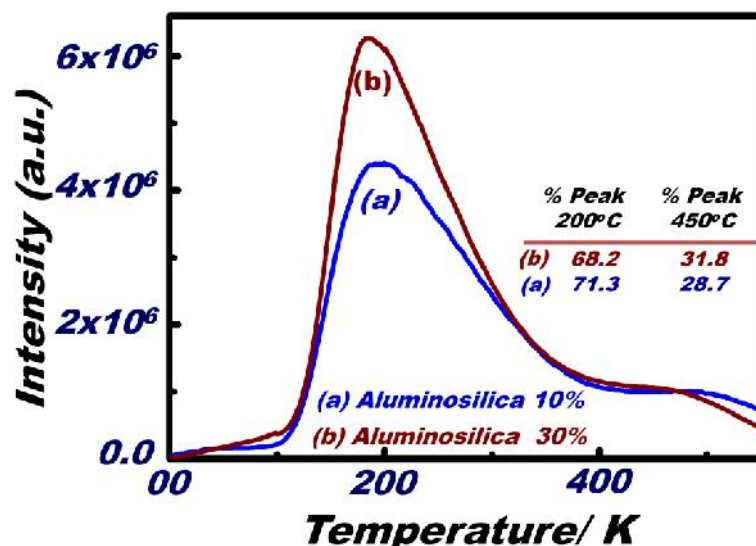


Fig. S6 NH₃-TPD spectra of calcined cubic Ia3d aluminosilica 10% (a) and aluminosilica 30% (b) monoliths

Growth inhibition by MASN under laboratory conditions

Radial growth technique has been used to check the potential of MASN for suppressing the development of *F. solani* compared with chinisol as a standard compound. The MASN and chinisol with various concentrations potentially suppress the development of *F. solani* in comparison with the control group. However, the highest growth inhibition percentage of

F. solani was achieved at the highest concentration (400 mg/L). The growth inhibition percentage of *F. solani* treated with chinisol ranged from 48 to 100 while for MASN 10 % ranged from 28.89- 79.66. Chinisol and MASN 10% were the most effective treatments against root rot fungus followed by MASN 30% (Table 1 and Fig. 1). MASN fungicidal activity against *F. solani* increased with increasing its concentration. MASN 10 % we found to be more effective against *F. solani* relative to MASN 30 %.

Table1 Growth inhibition percentages of the tested treatments against *F. solani* under laboratory conditions with regression equation and degree of correlation

Treatments	Concentration (mg/L)	Growth inhibition Percentage	Regression equation	R ²
MASN 10 %	100	28.89	Y= 0.1722x+13.22	0.99
	200	49.33		
	300	66.23		
	400	80.66		
MASN 30 %	100	13.89	Y=0.1669x-5.22	0.98
	200	26.22		
	300	41.45		
	400	64.44		
Chinisol	100	39.00	Y=0.2024x+22.1	0.98
	200	66.00		
	300	86.00		
	400	99.80		

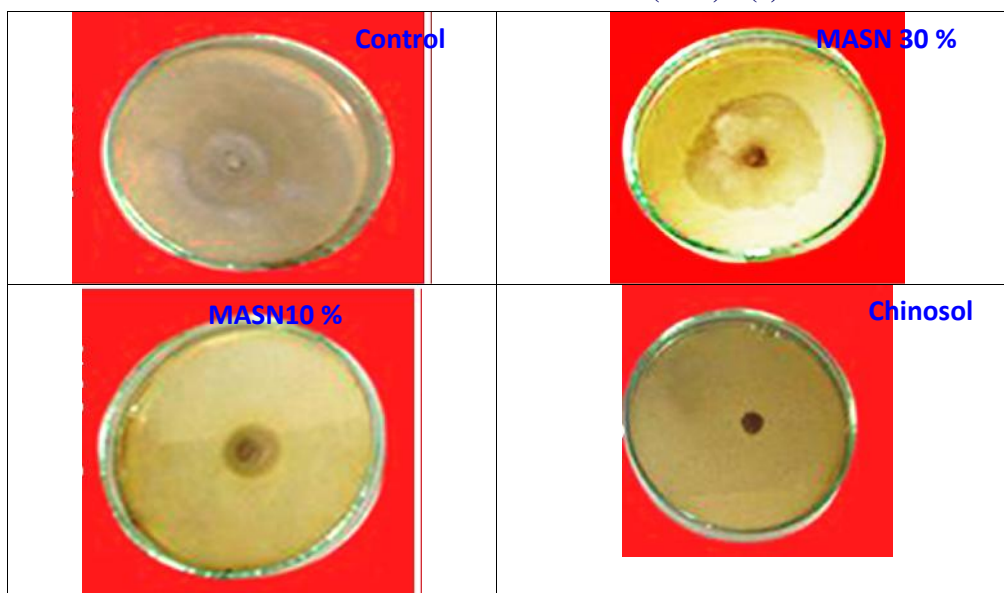


Fig. 1 Growth inhibition of *F. solani* under tested treatments compare to the control at concentration level of 400mg/l

Disease suppression MASN under greenhouse conditions

The efficacy of MASN was evaluated to check the ability of MASN to reduce the severity of *F. solani* on tomato compare to the standard or recommended compound (chinosol) under greenhouse conditions in two growing seasons. MASN and chinosol showed potential activity toward fusarium root rot of tomato plants relative to the untreated control group in both two seasons (Table 2). The highest efficacy (highest

percentage of survived plants) against root rot pathogen was for chinosol followed by MASN 10% and 30%, respectively (Table 2). The percentage of survived tomato plants treated with MASN and chinosol increased more than ten folds compare to untreated control in both growing seasons. The efficacy against root rot was better in the second season than in the first one. MASN 10% reduced the severity of root rot pathogen (high survival plants) higher than MASN 30 %.

Table 2 Efficacy of the tested treatments on root rot of tomato in both growing seasons under greenhouse conditions

Treatments	% Survived plants After 45 days	
	1 st season	2 nd season
Aluminasilica 10%	84.00±2.3b	88.00±2.12 b
Aluminasilica 30 %	68.00±2.88c	72.00±2.89 c
Chinosol	92.00±2.88a	96.00±2.95 a
Control	4.00±0.25d	8.00±0.35 d

Each value is mean of five replicates.

Mean ± SE followed by same letter in column of each treatment are not significant different at p = 0.05 as determined by Tukey–Kramer HSD.

Effect of MASN and chinosol on some growth characters of tomato

The effect of MASN compare to chinosol on some growth characters of tomato plants was investigated. The measured growth parameters were plant height as well as fresh and dry weights. The measured growth

characters were significantly increased in tomato plants treated with MASN and chinosol relative to untreated control. The highest growth parameters were recorded in tomato plants treated with MASN 10% followed by chinosol and MASN 30%, respectively (Table 3).

Table 3 Effect of the tested treatments on some growth parameters (plant height, fresh and dry weight) of tomato plants in season 2014

Treatments	Plant height (cm)	Fresh weight (g)	Dry weight (g)
Aluminasilica 10 %	99.00± 3.61de	54.00± 2.88 d	20.3±0.62 d
Aluminasilica 30 %	73.33±2.89 b	37.30±0.85 b	13.50±1.18 b
Chinosol	82.33±2.52c	44.67±2.05 c	13.37±0.45 b
Control	53.33±2.89 a	28.73±1.72 a	7.70±1.06 a

Each value is mean of four replicates. Mean ± SE followed by same letter in column of each treatment are not significant different at $p = 0.05$ as determined by Tukey–Kramer HSD.

Discussion

Soilborne diseases caused by several fungi such as *F. solani* can be a major limitation to crop production, particularly for vegetables. Soilborne pathogens often survive for long periods on host plant debris, soil organic matter, or as free-living organisms. They are often difficult to control, even with conventional strategies. Also these soilborne fungi became resistant to chemical fungicides. Therefore new safe and effective alternatives of fungicides to control plant pathogens such as root rot of tomato considered a source of major concern. The concept of utilizing nanoparticles as an antimicrobial agent is comparatively new, as the focus has now been shifted towards making non-toxic, safe nanoparticles (Tank et al., 2013). The tested MASN significantly reduced the severity of *F. solani*, the causative fungus of root rot of tomato relative to the control. The fungicidal effect of some metal oxides nanoparticles such as ZnO and CuO, has been reported previously for some plant diseases caused by fungi, such as *Fusarium* sp. and *Alternaria* sp. (Wani and Shah, 2012). MASN nanoparticles synthesized via simple one-pot microemulsion polymerization method gave uniform size distribution as indicated by X-RD result. Besides, the high surface area (S_{BET}) of $387\text{m}^2/\text{g}$ and small pore size (D_p) of 10.4 nm of MASN confirmed by XRD and Nitrogen isotherms. All these characters improve the significance of the surface morphology of the MASN nanoparticles participating in the cellular interaction i.e., the number of active sites coming in contact with

the cells which render cytotoxic effect against root rot fungus. Also, it is well known that the smaller particles have larger surface area available for interaction and will give more antimicrobial effect than the larger particles. The higher efficacy MASN 10 % than MASN 30% against *F. solani* either under laboratory or greenhouse conditions may be due to its high surface area and small particle size relative to MASN 30% (Fig. S1).

The mode of action of any control agents are very important and help in improving the efficacy of it when we faced some defects of its efficacy. The mechanism of MASN action against *F. solani* is not clearly known till now but there are many theories in this regard. Many hypotheses were supposed to explain the fungicidal activity of MASN (Fig.2), such as the inhibition of enzymes and toxins utilized by the fungi to induce pathogenesis (Bhainsa and D'Souza, 2006; Vahabi et al., 2011). Further, the interface of MASN with protein molecules inactivates the protein molecules and may cause a mutation in the DNA that blocks its replication potential (Petica et al., 2008; Salem et al., 2011). In another scenario, the small particle size of MASN contributed to its facile penetration in the cell wall (cell membrane) and accumulation in the cell membrane causing cell lysis (Gill et al., 2005). Moreover, MASN may deactivate transmembrane energy cycle through the presence of insoluble compounds in the cell wall and interrupt its electron transport series. In addition, the high aluminum content increase the positive charge on

aluminasilica surface and the positive charge is the key parameter in aluminasilica action against root rot fungus. Since the fungal cell having negative charges (thiol groups (-SH) of the proteins present on the microbial cell surface) induced electromagnetic

attraction between the MASM (positive charge) and the fungal cell. This led to oxidation of the fungal cell, and subsequently, cell death (Zhang and Chen, 2009; Rezaei-Zarchi et al., 2010).

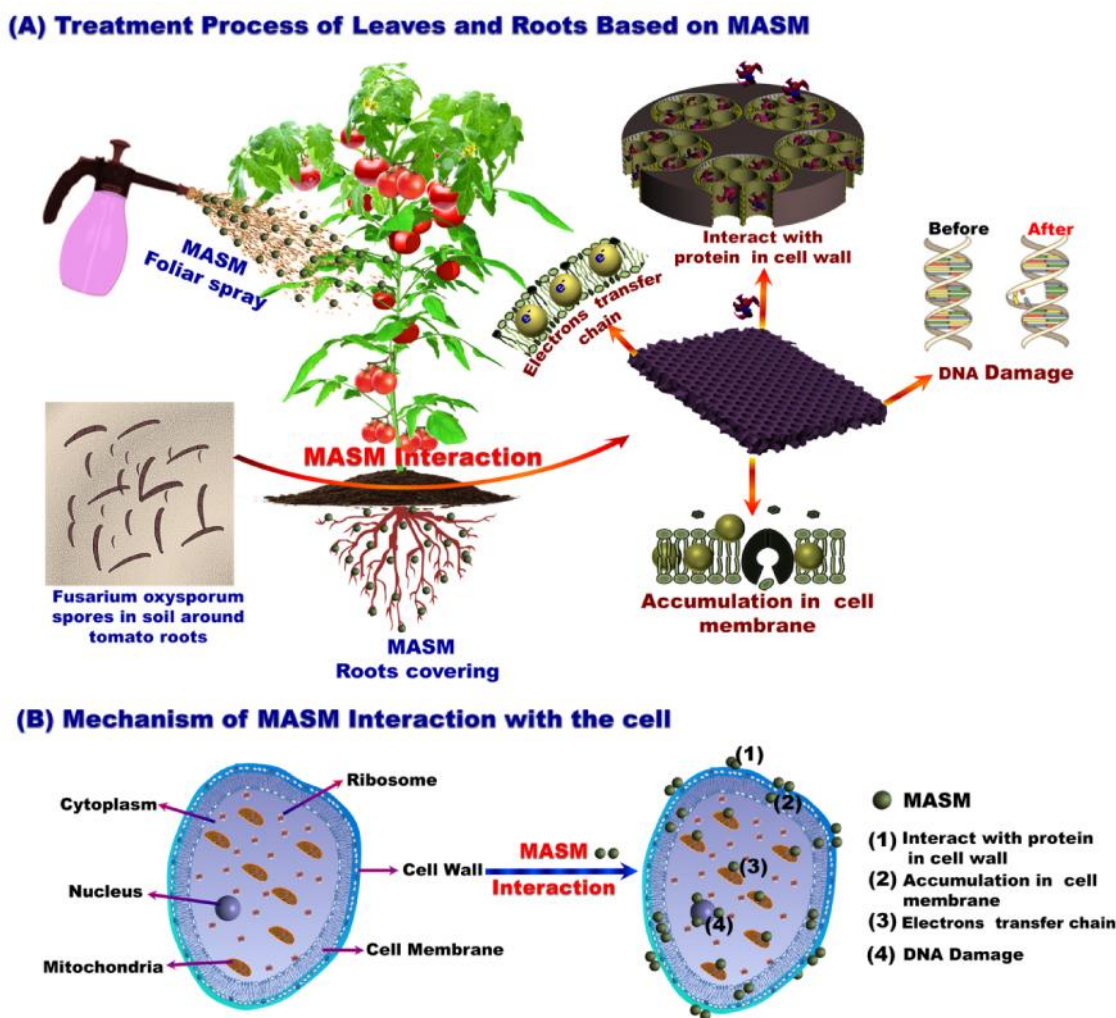


Fig.2 Schematic representation of various mechanisms (cell membrane interaction, DNA damage, protein interaction in cell wall, interruption electron transfer chain, suppression of enzymes or toxins used by *F. solani* for pathogenesis) of antifungal activity of MASN-NPs

The potential effect of MASN toward root rot of tomato may be due to the absorption of silicon (Si) presented as a component in MASN in plants. This might increase the disease and stress resistance of the treated plants besides suppressing the fungus itself (Brecht et al., 2003; Ma et al., 2001). Furthermore, the excellent preventive effects of aqueous silicate solution on plant pathogenic microorganisms and the promotion in the physiological activity and plant growth strongly support this approach (Garver et al., 1998; Kanto et al., 2004).

Also, one of the most important factors is the amount of MASN that could be used under field conditions and it is suitable and applicable or not. The amount needed from MASN to spray one acre depend on our results if we supposed that one acre need 100 L water may be 40 g /4046.85 m². We think, this amount is applicable and comparable to the tested fungicide amount (30 g /4046.85 m²) and cost effective.

The physical mechanism of MASN strongly suggests its use as a solution to fungi resistance, wherein the fungi are most unlikely to become genetically and physiologically resistant to such mode of action. Moreover, this antifungal activity of MASN has several targets in attacking the fungal cell, which needs several mutations in the fungi to protect themselves. Thus, the fungi cannot become resistant to MASN as induced against chemical fungicides (Pal et al., 2007). Moreover, the physical mode of action of MASN against *F. solani* makes it not specific to this fungus only which strongly supports the use of MASN against other plant pathogens.

Growth and yield characters of crops should be taken in consideration when we try to find and evaluate new control agents against agricultural pests. The control agents should not negatively affect the growth and yield parameters of the crop. The results of our study showed significant increase in tomato growth parameters under different treatments relative to the control. This may be because the MASN and chinosol reduced the damaged leaf area caused by the fungus, thereby increasing plant growth due to longer photosynthesis in leaves (Paveley et al., 1997) and subsequently increasing growth and yield of tomato (EL-Mougy et al., 2013). Also, the increased growth parameters of tomato plants treated with MASN may be due to that alumina content in MASN that known to increase photosynthetic quantum yield of photosystem II under steady state conditions (Govorov and Carmeli, 2007). The increase in photosystem II subsequently increases photosynthesis process and plant growth characters.

The safety of new materials that used for control agricultural pests as alternatives to chemical pesticides considered a source of major concern. Not only the potential effect of these control agents against pests but also its safety is needed and it considered limiting factor for traditional application. MASN has considerable efficacy against *F. solani*. Results effectively propose a synthetic compound based on biological effects of nanoparticles for treating root rot disease caused by different species of Fusarium fungus.

Conflict of Interest Statement

No conflict of interest

References

- Ainsworth G.C., and James P.W. (1971): Ainsworth and Bishy's Dictionary of fungi. 6th ed. Commonwealth Mycological Institute, Kew, Surrey, UK. pp 663.
- Alexopoulos C.J., Mims C.W., Blackwell M.M. (1996): Introductory To Mycology. 6th ed. John Wiley.
- Bai, P., Wu, P., Yan, Z., and Zhao X. S. (2009): Cation–anion double hydrolysis derived mesoporous γ - Al_2O_3 as an environmentally friendly and efficient aldol reaction catalyst. Journal Materials Chemistry, 19: 1554-1563
- Bhainsa, K.C., and D'Souza, S.F. (2006): Extracellular biosynthesis of silver nanoparticles using the fungus *Aspergillus fumigatus*. Colloids Surface B Biointerfaces, 47: (2) 160-164.
- Brecht M., Datnoff L., Nagata R., and Kucharek T. (2003): The role of silicon in suppressing tray leaf spot development in St. Augustine grass. Publication in University of Florida, 1-4.
- Che S., Garcia-Bennett A., Yokoi T., Sakamoto K., Kunieda H., Terasaki O., and Tatsumi T. (2003): A novel anionic surfactant templating route for synthesizing mesoporous silica with unique structure. Nature Materials, 12: 801-805.
- Climent M.J., Corma A., Iborra S., Navarro M.C., and Primo J. (1996): Use of mesoporous mcm-41 aluminosilicates as catalysts in the production of fine chemicals-preparation of dimethylacetals. Journal Catalysis, 161: (2) 783-789.
- Das S.k., Kapoor S., Yamada H., and Bhattacharyya A. J. (2009): Effects of surface acidity and pore size of mesoporous alumina on degree of loading and controlled release of ibuprofen. Microporous Mesoporous Materials 118: 267-272.
- Derbalah A., El-Safty S.A., Shenashen M.A., and Abdel Ghany N.A. (2015): Mesoporous alumina nanoparticles as host tunnel-like pores for removal and recovery of insecticides from environmental samples. Chem Plus Chem, 80: (7) 1119-1126.
- Dhingra O.D., Sinclair J.B. (1995): Basic plant pathology methods. Second Edition, CRC Press, Inc. pp. 434.
- Du H., Terskikh V.V., Ratcliffe C.I., and Ripmeester J.A. (2002): Distinguishing surface versus buried cation sites in aluminosilicate mesoporous materials. Journal American Chemical Society, 124: 4216-4217.
- Duncan D.B., 1955. Multiple range and multiple F-test. Biomatrix, 11: 1-42.

- El-Mohamedy R.S.D., Jabnoun-Khiareddine H., and Mejda Daami-Remadi M. (2014):** control of root rot diseases of tomato plants caused by *Fusarium solani*, *Rhizoctonia solani* and *Sclerotium rolfsii*. Tunisian Journal of Plant Protection, 9: (1) 45-55.
- El-Mougy N.S., Abdel-Kader M.M., Lashin S.M., and Megahed A.A. (2013):** Fungicides alternatives as plant resistance inducers against foliar diseases incidence of some Vvegetables grown under plastic houses conditions. International Journal of Engineering and Innovation Technology, 3: (6) 71-81.
- El-Safty S.A., and Hanaoka T. (2003):** Fabrication of crystalline, highly ordered three-dimensional silica monoliths (HOM-n) with large, morphological mesopore structure. Advanced Materials 15: 1893-1899.
- El-Safty S.A., Sakai M., Selim M.M., and Alhamide A.A. (2015):** One-pot layer casting-guided synthesis of nanospherical aluminosilica@organosilica@alumina core-shells wrapping colorant dendrites for environmental application. RSC Advances , 5: (74) 60307-60321.
- El-Safty S.A., Shenashen M.A., Ismael M., Khairy M., and Awual M.R. (2013):** Mesoporous aluminosilica sensors for the visual removal and detection of Pd (ii) and Cu(ii) ions. Microporous and Mesoporous Materials, 166: 195-205.
- El-Safty S.A., Shenashen M.A., Ismael M., and Khairy M. (2012):** Mesocylindrical aluminosilica monolith biocaptors for size-selective macromolecule cargos. Advanced Function Materials, 22: (14) 3013-3021.
- El-Safty S.A., Mekawy M., Yamaguchi A., Shahat A., Ogawa K., and Teramae N. (2010):** Organic-inorganic mesoporous silica nanostrands for ultrafine filtration of spherical nanoparticles. Chemistry Communication, 46: 3917-3919.
- El-Safty S.A., Shenashen M.A., and Shahat A. (2013):** Tailor-made micro-object optical sensor based on mesoporous pellets for visual monitoring and removal of toxic metal ions from aqueous media. Small, 9: (13) 2288-2296.
- El-Safty S.A., and Hanaoka T. (2004):** Microemulsion liquid crystal templates for highly ordered three dimensional mesoporous silica monoliths with controllable mesopore structures. Chemistry Materials, 16: 384-400.
- El-Safty S.A., Hanaoka T., and Mizukami F. (2005):** Transparent cubic Fd3m mesoporous silica monoliths with highly controllable pore architectures. Journal Materials Chemistry, 15: 2590-2598.
- El-Safty S.A., Hanaoka T., and Mizukami F. (2005):** Large-scale design of cubic Ia3d mesoporous silica monoliths with high order, controlled pores, and hydrothermal stability. Advanced Materials, 17: 47-53.
- El-Safty S.A., Kiyozumi Y., Hanaoka T., and Mizukami F. (2008):** Cationic surfactant templates for newly developed cubic Fd3m silica mesopore structure. Materials Letter , 62: 2950-2953.
- El-Safty S.A., Shahat A., and Ismael M. (2012):** Mesoporous aluminosilica monoliths for the adsorptive removal of small organic pollutants. Journal of Hazardous Materials, 201: 23-32.
- Esfahani M.N. (2006):** Present status of Fusarium dry rot of potato tubers in Isfahan (Iran). Indian Phytopathology, 59: (2) 142-147.
- Esfahani M., Perez-de-Luque N., and Diego A.R. (2009):** Nanotechnology for parasitic plant control. Pest Management Science, 65: 540-545.
- Garcia-Bennett A.E., Lund K., and Terasaki O. (2006):** Particle-size control and surface structure of the cubic mesopore material AMS-8. Angew Chemistry Institute Ed 45: (15) 2434-2438.
- Garver T.L.W., Thomas B.J., Robbins M.P., and Zeyen R.J. (1998):** Phenylalanine ammonia-lyase inhibition, auto fluorescence, and localized accumulation of silicon, calcium and manganese in oat epidermis attacked by the powdery mildew fungus *Blumeria graminis* (DC) speer. Physiology Molecular Plant Pathology, 52: 223- 243.
- Gill S., Fouts D.E., Archer G.L., Mongodin E.F., Deboy R.T., Ravel J., Paulsen I.T., Kolonay J.F., Brinkac L., Beanan M., Dodson R.J., Daugherty S.C., Madupu R., Angiuoli S.V., Durkin A.S., Haft D.H., Vamathevan J., Khouri H., Utterback T., Lee C., Dimitrov G., Jiang L., Qin H., Weidman J., Tran K., Kang K., Hance I.R., Nelson K.E., and Fraser C.M. (2005):** Insights on evolution of virulence and resistance from the complete genome analysis of an early methicillin-resistant staphylococcus aureus strain and a biofilm-producing methicillin-resistant *Staphylococcus epidermidis* strain. Journal Bacteriology, 187: 2426-2438.
- Giovannucci E. (1999):** Tomatoes tomato-based products, lycopene and cancer: Review of the epidemiologic literature. Journal Natural Cancer Institute 91: 317-331.
- Hadian S.H., Shamluo P., Monazam K., and KHanduoz A. (2011):** Effect of aqueous extracts of medicinal plants against *F. oxysporum f.sp. lycopersici* Pzmrddy operating tomatoes. Journal of Plant Science, 6: (21) 68-77.

- Juhela G., Batissea E., Huguesa Q., Dalya D., Van Peltb F.N.A.M., O'Hallorana J., and Marcel Jansena A.K. (2011):** Alumina nanoparticles enhance growth of *Lemna minor*. *Aquatic Toxicology*, 105: 328-336
- KKhalifa E.Z. (1987):** Further studies on some soil-borne fungi affecting soybean and their control. Ph.D. Thesis, Faculty of Agriculture Menoufiya University Egypt, 148 pp.
- Kanto T., Miyoshi A., Ogawa T., Maekawa K., and Aino M. (2004):** Suppressive effect of potassium silicate on powdery mildew of strawberry in hydroponics. *General Plant Pathology*, 70: 207-211.
- Kern A., Coelho A.A., and Cheary R.W. (2004):** Convolution based profile fitting, diffraction analysis of the microstructure of materials" Edited by Mittemeijer E. J.; Scardi, P., *Materials Science*, 17-50.
- Khairy M., and El-Safty S.A. (2014):** Hemoproteins–nickel foam hybrids as effective super capacitors. *Chemical Communication* 50: (11) 1356-1358.
- Kumar V., and Yadav S.K. 2009. Plant-mediated synthesis of silver and gold nanoparticles and their applications. *Journal Chemistry Technology Biotechnology*, 84: 151–157.
- Lambert J.F., Millman W.S. and Fripiat J.J. (1989):** Revisiting kaolinite dehydroxylation: a silicon-29 and aluminum-27 MAS NMR study. *Journal American Chemical Society* 111: 3517-3522.
- Linssen T., Mees F., Cassiers K., Whittake A., and Vansant E.F. (2003):** Characterization of the acidic properties of mesoporous aluminosilicates synthesized from leached saponite with additional aluminum incorporation. *Journal Physical Chemistry, B* 107: 8599-8606.
- Lippmaa E., Samoson A., and Mägi M. (1986):** High-resolution aluminum-27 NMR of aluminosilicates. *Journal American Chemistry Society*, 108: 1730 -1735.
- Lui Y., Zhang W., and Pinnavaia T.J. (2000):** Steam-stable aluminosilicate mesostructures assembled from zeolite type Y seeds. *Journal American Chemistry Society*, 122: 8791-8792.
- Ma J.F., Goto S., Tami K., and Ichii M. (2001):** Role of root hairs and lateral roots in silicon uptake by rice. *Plant Physiology*, 127: 1773-1780.
- Pal S., Tak Y.K., and Song J.M. (2007):** Does the antibacterial activity of silver nanoparticles depend on the shape of the nanoparticle? A study of the gram-negative bacterium *Escherichia coli*. *Applied Environmental Microbiology*, 73:1712–1720.
- Paveley N.D., Lockley K.D., Sylvester-Bradley R., and Thomas J. (1997):** Determination of fungicide sprays decisions for wheat. *Pesticide Science*, 49: 379–88.
- Petica A., Gavrilu S., Lungu M., Buruntea N., and Panzaru C. (2008):** Colloidal silver solutions with antimicrobial properties. *Materials Science and Engineering*, 152: (1–3) 22–27.
- Platschek B., Petkov N., and Bein T. (2006):** Tuning the structure and orientation of hexagonally ordered mesoporous channels in anodic alumina membrane hosts: a 2D small-angle X-ray scattering study. *Angew Chemical International*, Ed 45: 1134-1138.
- Rezaei-Zarchi S., Javed A., Ghani M.J., Soufian S., Firouzabadi F.B., Moghaddam A.B., and Mirjalili S.H. (2010):** Comparative study of antimicrobial activities of TiO₂ and CdO nanoparticles against the pathogenic strain of *Escherichia coli*. *Iran Journal Pathology*, 5: (2) 83-89.
- Salem H.F., Eid K., and Sharaf M. (2011):** Formulation and evaluation of silver nanoparticles as antibacterial and antifungal agents with a minimal cytotoxic effect. *International Journal of Drug Delivery*, 3: 293–304.
- Shen S., and Kawi S. (1999):** Uunderstanding of the effect of Al ssubstitution on the hhydrothermal sstability of MCM-41. *Journal Physical Chemistry, B*, 103: 8870-8876.
- Shenashen M.A., El-Safty S.A., and Elshehy E.A. (2014):** Monolithic scaffolds for highly selective ion sensing removal of Co(ii) Cu (ii) and Cd (ii) ions in water. *Analyst*, 139: (24) 6393-6405.
- Shenashen M.A., El-Safty S.A., Elshehy E.A., and Khairy M. (2015):** Hexagonal –prism-shaped optical sensor/captor for optical recognition and sequestration of Pd ions from urban mines. *European Journal of Inorganic Chemistry*, 1: 179-191.
- Shenashen M.A., El-Safty S.A., and Khairy M. (2013c):** Trapping of biological macromolecules in the three-dimensional mesocage pore cavities of monoliths adsorbents. *Journal of Porous Materials*, 20: (4) 679-692.
- Shenashen M.A., Elshehy E.A., El-Safty S.A., and Khairy M. (2013a):** Visual monitoring and removal of divalent copper cadmium and mercury ions from water by using mesoporus cubic Ia3d aluminasilica silica. *Seperation and Purification Technology*, 116: 73-86.

Shenashen M.A., El-Safty S.A., and Elshehy E.A.

(2013b): Architecture of optical sensor of optical sensor for recognition of multiple toxic metal ions from water. *Journal of Hazardous Materials*, 260: 833-843.

Shigeno T., Inoue K., Kimura T., Naonbu K.,

Niwa M., and Kuroda K. (2003): Synthesis and stability studies of conformationally locked 4-(diaryl-amino) aryl- and 4-(dialkyl-amino) phenyl-substituted second-order nonlinear optical polyene chromophores. *Journal Materials Chemistry B*, 13: 825- 883.

Vahabi K., Mansoori G.A., Karimi S. (2011):

Biosynthesis of silver nanoparticles by fungus *Trichoderma Reesei*. *Inscience Journal*, 1: 65-79.

Vincent J.H. (1947): Distortion of fungal hyphae in

presence of certain inhibitor. *Nature* 15: 850.

Wang Y., Lang N., and Tuel A. (2006): Nature and

acidity of aluminum species in AlMCM-41 with a high aluminum content (Si/Al = 1.25). *Microporous Mesoporous Materials*, 93: (1-3) 46-54.

Wani A.H., and Shah M.A. (2012): A unique and

profound effect of MgO and ZnO nanoparticles on some plant pathogenic fungi. *Journal Applied Pharmaceutical Science*, 02: (03) 40-44.

Xia J., Mao D., Tao W., Chen Q., Zhang Y., and

Tang Y. (2006): Dealumination of HMCM-22 by various methods and its application in one-step synthesis of dimethyl ether from syngas. *Microporous Mesoporous Materials*, 91: 33-39.

Zhang H., and Chen G. (2009): Potent antibacterial

activities of Ag/TiO₂ nanocomposite powders synthesized by a one-pot sol-gel method. *Environmental Science Technology*, 43: (8) 2905-2910.

Access this Article in Online	
	Website: www.ijarbs.com
	Subject: Nanotechnology
<p style="text-align: center;">Quick Response Code</p>	
DOI: 10.22192/ijarbs.2017.04.06.017	

How to cite this article:

M. Shenashen; A. Derbalah; A. Hamza; A. Mohamed , S. El Safty. (2017). Recent trend in controlling root rot disease of tomato caused by *Fusarium Solani* using aluminasilica nanoparticles. *Int. J. Adv. Res. Biol. Sci.* 4(6): 105-119.

DOI: <http://dx.doi.org/10.22192/ijarbs.2017.04.06.017>